ORNL/TM-2024/3253

Report on Initial Tribological Studies of Graphite in Dry Argon and Molten Salt Environment

Tomas Grejtak
Jun Qu
Nidia C. Gallego
James R. Keiser

January 2024

OAK RIDGE National Laboratory

ORNL IS MANAGED BY UT-BATTELLE LLC FOR THE US DEPARTMENT OF ENERGY

ORNL/TM-2024/3253

Materials Science and Technology Division
Chemical Science Division

REPORT ON INITIAL TRIBOLOGICAL STUDIES OF GRAPHITE IN DRY ARGON AND MOLTEN SALT ENVIRONMENT

Tomas Grejtak
Jun Qu
Nidia C. Gallego
James R. Keiser

January 2024

Prepared by
OAK RIDGE NATIONAL LABORATORY
Oak Ridge, TN 37831
managed by
UT-BATTELLE LLC
for the
US DEPARTMENT OF ENERGY
under contract DE-AC05-00OR22725

CONTENTS

LIST OF FIGURES

LIST OF TABLES

ACKNOWLEDGMENTS

This work was supported by the US Department of Energy, Office of Nuclear Energy, Advanced Reactor Technology Program.

The authors would like to thank Ryan Latta and Gabriel Meric from Kairos Power LLC for providing us with graphite pebbles and for their discussion on operational parameters of a molten salt reactor. The authors are also grateful to Kevin Cooley and Daniel Fleming for machining the graphite samples used in this work, Adam Willoughby for setting up the glovebox and Wenbo Wang for helping to set up the tribometer.

ABSTRACT

This report documents completion of the Advanced Reactor Technologies (ART) Level 2 Milestone M2TG-24OR0501081: "Complete report on initial tribological studies within molten salt environment", due January 31, 2024. This milestone is a carryover milestone from FY23 M2TG-23OR0501091. The report summarizes the initial studies on tribological characterization of the graphite–graphite sliding interface in a dry argon and molten FLiNaK salt environment. The experiments were conducted on a high-temperature multifunctional tribometer placed in a glovebox. This configuration enables probing the wear and friction properties at high temperatures in an inert environment. The worn surfaces were analyzed using high-resolution microscopy and white-light profilometry to determine the wear modes and wear rates. This report discusses the previous wear and friction studies on 316H stainless steel (SS) sliding against graphite in molten salt for different temperatures, sliding speeds, and salt amount. Moreover, key tribological parameters of pebble-on-pebble interaction in gas-cooled and molten salt reactors (MSRs) are analyzed and used to design an experimental test matrix for future studies. The outcomes of this project could provide key information about the tribological behavior of graphite pebbles in gas-cooled and MSRs, thereby contributing to safer operation.

1. INTRODUCTION

High temperature gas-cooled pebble bed reactors (HTGRs) and MSRs contain thousands of densely packed fuel pebbles that pass slowly through the reactor core multiple times before they are finally discharged [1], [2], [3], [4], [5]. The pebbles have a spherical shape and are typically 4–6 cm in diameter. Each pebble contains microfuel particles that are encapsulated by a thin (hundreds of micrometers) carbon composite outer shell and embedded in an outer graphite matrix shell [6]. HTGRs and MSRs typically operate at temperatures up to 700°C [2], [4]. In HTGRs, an inert gas, typically helium, passes through the pebbles and serves as a coolant. During operation, the pebbles move from top to bottom of the reactor by the force of gravity, as illustrated in Figure 1a. The fuel pebbles in an MSR move very differently from those in an HTGR. Molten salt, which serves as a coolant, circulates from bottom to top, as shown in Figure 1b [1], [2]. Graphite pebbles are less dense than molten salt and are positively buoyant; therefore, they flow in the same direction as the molten salt.

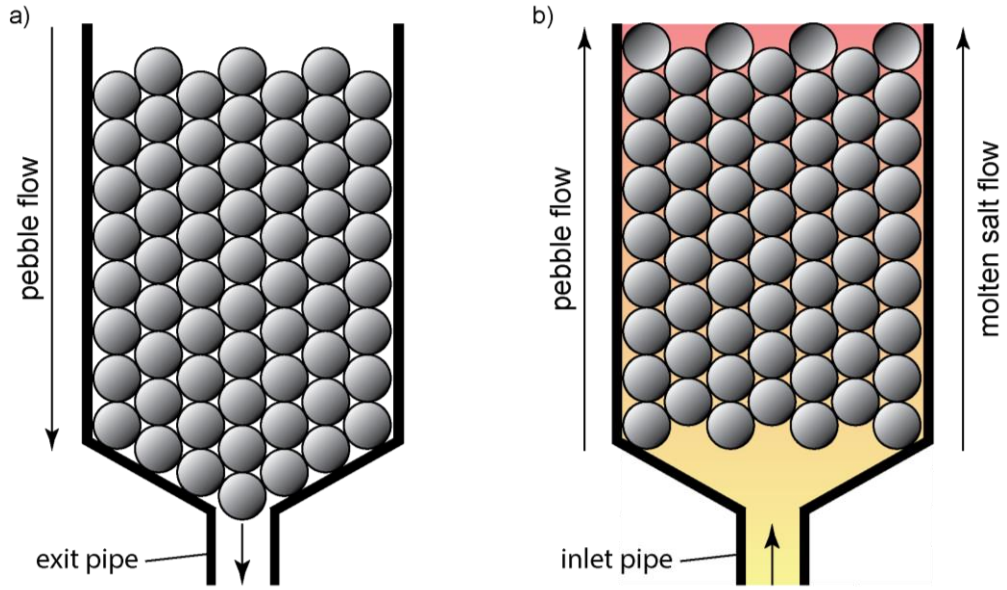

Figure 1. Schematic of high temperature reactors. (a) Gas-cooled pebble bed reactor. (b) Molten salt reactor.

As pebbles circulate through the reactor, they contact other pebbles, graphite wall blocks, and the metallic containment reactor components. This contact causes their abrasion [7], [8]. Graphite dust particles may be contaminated with fission products, presenting another safety hazard. Dust forms in both HTGRs and MSRs and can negatively affect their operation. Therefore, understanding the tribological properties and behavior of graphite pebbles is important for estimating their service life and dust generation.

The wear and friction properties of graphite have been studied for decades. The primary wear modes in graphite-on-graphite sliding are adhesive and abrasive wear [9], [10], [11]. The tribological properties strongly depend on the environment. In general, sliding in an environment containing reactive species such as oxygen and hydrogen results in lower friction and wear than sliding in a vacuum [9], [11]. Adsorption of these reactive species reduces adhesion, which essentially reduces the interfacial shear strength. Friction and wear also tend to decrease with increasing temperature. Graphite gets stronger as temperature increases, improving the abrasion and adhesion resistance. Graphite-on-graphite sliding in dry (unlubricated) conditions enables formation of a tribofilm that has a lubricating effect [9], [10], [11]. A tribofilm is formed by redepositing wear debris that formed during sliding. Higher temperatures enable thicker and more continuous tribofilm.

Several studies attempted to study tribological performance of graphite in an argon environment [9], [10], [12]. However, very few studies focused on tribological characterization of graphite with conditions that are relevant to the nuclear reactor. Vergari et al. [10] studied the wear and friction properties of nuclear graphite ET-10 in an argon environment for a range of temperatures from room temperature up to 600°C. The data showed that the lower friction and wear rate are achieved at higher temperatures. This result was attributed to the formation of a stable tribofilm and lower interfacial adhesion. A very ambitious study by Shen et al. [13] examined the abrasion behavior of a graphite pebble in an SS lifting pipe during the circulation process at different velocities and different gas atmospheres. The abrasion rate increased with increasing velocities owing to more frequent collisions between the pebbles and the lifting pipe.

Several studies investigated tribocorrosion of different alloys in molten salt [14], [15], [16]. One of the more recent studies involved tribological characterization of graphite pins sliding against 316H SS disks lubricated by a ternary eutectic fluoride molten FLiNaK salt in an argon environment [17]. This work examined the tribological behavior of graphite pebbles when they contact the SS container wall during circulation. This comprehensive study investigated the wear and friction properties for key parameters such as temperature, normal load, and salt amount. The key findings from these efforts are discussed in this report.

The goal of the work presented in this report is to investigate the tribological behavior of graphite pebbles in HTGRs and MSRs by determining the key parameters of the pebble motion in the reactor during circulation. These parameters will then be used to design a test matrix to characterize and predict the wear and friction properties of graphite materials in conditions that closely resemble those in HTGRs and MSRs.

First, initial tribological studies were performed on graphite in a dry argon environment (unlubricated) and molten FLiNaK salt lubricated conditions. Graphite samples were machined from a graphite pebble provided by Kairos Power LLC. The wear and friction properties were investigated using a pin-on-disk configuration in an argon environment at 650°C. The experiments were conducted on a multifunctional high-temperature tribometer that was placed in a glovebox to ensure environmental control. The data analysis includes the wear rate and evolution of the coefficient of friction (COF) over sliding distance. The wear mechanism was evaluated using optical microscopy, white-light profilometry, scanning electron microscopy (SEM), and energy dispersive spectroscopy (EDS). The results were compared with those of similar tests from other studies. Friction data from tribological testing in dry argon conditions show good

agreement with the data from Vergari et al. [10]. A literature search reveals no existing data on tribological behavior of graphite-on-graphite sliding in molten salt.

The second part of this report analyzes the tribologically relevant conditions of the pebbles' interactions in HTGRs and MSRs. Understanding key parameters such as gas environment, temperature, contact motion, contact load, sliding and rolling speed and distance are crucial for designing the test matrix. Unfortunately, the literature does not provide sufficient information on dynamic interactions of pebbles. Reviewed experimental studies on tribological properties of graphite in an HTGR did not provide justification for selecting certain key test parameters [5], [10]. For this report, the parameters such as pebble-on-pebble contact load/pressure, sliding and rolling distance and speed, and temperature were analyzed and determined based on inputs from the modeling results from Tang et al. [3] and from internal communication with Kairos Power.

When this study is completed, the results will provide key information about the underlying mechanism of pebbles rubbing against each other and the estimated wear rate. This information is essential for evaluating the integrity and service life of a graphite pebble and ensuring safe operation of the reactor. With more success, the outcomes of this work could be used to characterize the dust and predict its generation during pebble circulation.

2. EXPERIMENTAL PROCEDURE

2.1 SAMPLE PREPARATION

The test specimens for tribological testing were machined from graphite pebbles with a diameter of 40 mm provided by Kairos Power, as shown in Figure 2. Two specimen geometries were fabricated: a flat square disk (25.4 × 25.4 × 1.6 mm) and a pin with a cylindrical diameter of 9.42 mm and a 40 mm tip diameter. Disk specimens were polished using silicon carbide papers of 400, 600, and 800 grit to a final roughness of ~0.2 µm (R_a). The as-received surface roughness of the pin for testing in dry argon unlubricated conditions was ~5.5 µm (R_a) and ~11.8 µm (R_a) for tests conducted in molten salt. Before experimental testing, the test specimens were sonicated in isopropanol for 30 min. Commercial fluoride molten FLiNaK (LiF:NaF:KF;46.5:11.5:42 mol %) salt purchased from Materion Advanced Chemicals Inc. was selected for this study.

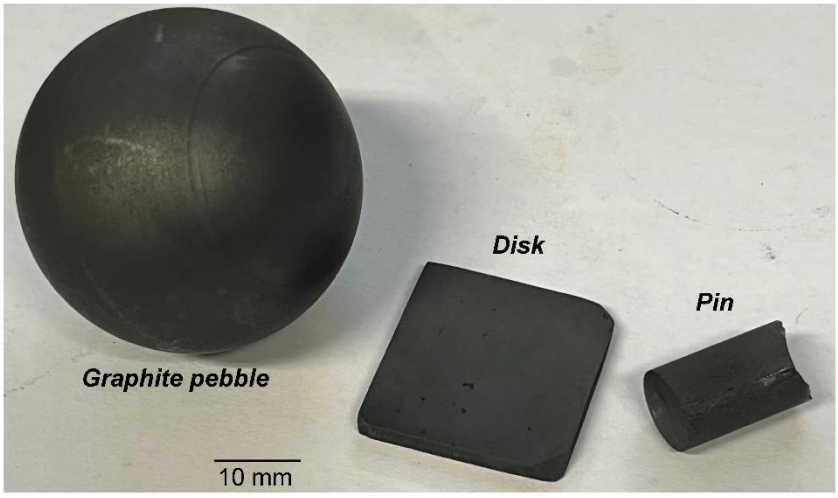

Figure 2. Graphite pin and disk used in the experiments were fabricated from a graphite pebble.

2.2 TRIBOLOGICAL TESTING

2.2.1 Multifunctional Tribometer

The tribological experiments were performed on a multifunctional tribometer (Rtec MFT-2000A), as shown in Figure 3a. The tribometer consists of a vertical loading head (loading range 1–200 N), a rotary stage (maximum speeds up to 2,500 rpm), a linear *x*-*y* stage, and a high-temperature furnace with temperature capability up to 1,000°C. The current capabilities enable testing using a pin-on-disk configuration. In this setup, the graphite pin is attached to a sample holder that is mounted to a vertical load head, and the graphite disk is mounted to a rotary stage, as shown in Figure 3b. The apparatus is also equipped with an imaging system that consists of an optical microscope, a white-light profilometer, and a confocal microscope, as shown in Figure 3c. The tribometer was placed in a glovebox to allow testing in an inert argon environment at high temperatures to prevent oxidation of graphite samples, as shown in Figure 4.

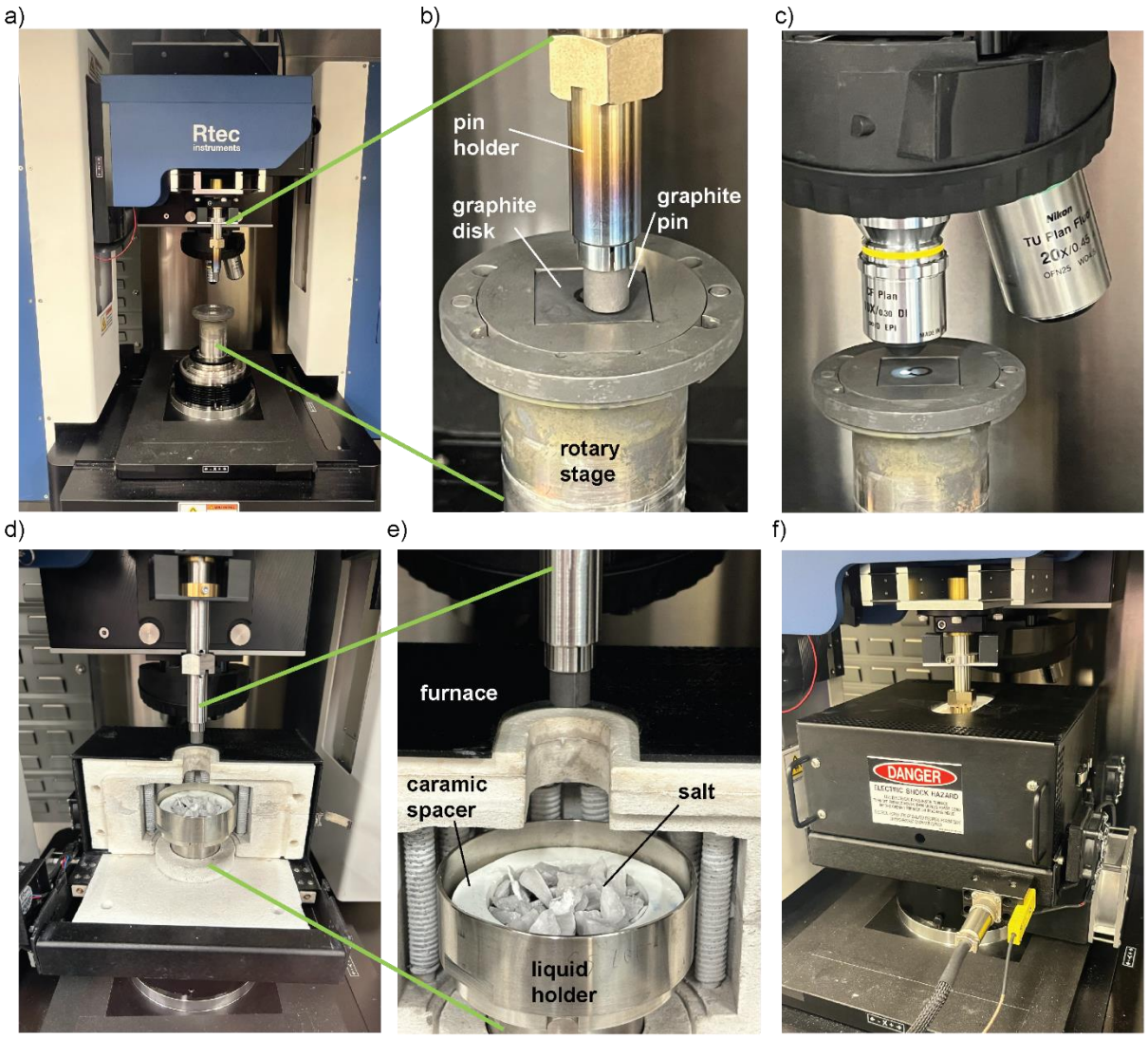

Figure 3. Experimental setup. (a) Multifunctional tribometer. (b) Dry sliding test setup. (c) White-light profilometer. (d) Molten FLiNaK salt wear test setup. (e) Detail view showing a liquid holder loaded with salt on top of a graphite disk. (f) The liquid and pin holder contained within a high-temperature furnace.

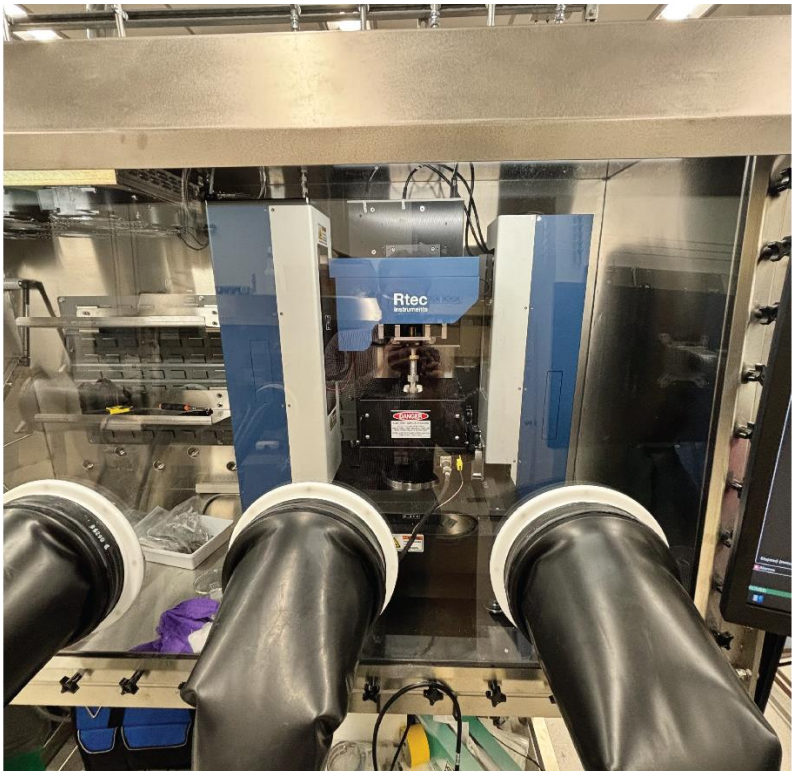

Figure 4. Tribometer placed in a glovebox filled with argon gas.

2.2.2 Test Parameters and Design

The test conditions used in this study were similar to those used in the previous work on 316H SS sliding on graphite in molten FLiNaK salt [17]. Similar test conditions were used for tribological experiments in dry argon and molten salt environments. The normal load was set to 20 N, and the temperature inside the chamber was held constant at 650°C. The tribological performance in dry argon conditions was tested at two different speeds: 1 mm/s and 10 mm/s. A molten FLiNaK salt lubricated test was performed only at the 10 mm/s sliding speed. The total sliding distance was 10 m. Both dry argon and molten salt lubricated tests were performed in an argon atmosphere. The moisture and oxygen content were <1 ppm. About 13 g of salt were used for a molten salt lubricated test. The COF was recorded in situ. After the experiments were complete, the worn-surface morphology and topography of the pin and the disk were examined using the optical microscope and the white-light profilometer.

Current capabilities of the tribometer enable testing in dry (Figure 3b) and liquid (Figure 3d,e) environments. Both conditions require using different disk sample holders. Figure 3b shows a setup for tests that were conducted in dry argon environment. After the test was complete, the pin was retracted from the furnace, but the disk was kept in the furnace and allowed to cool.

Testing in liquid requires a special disk holder, as shown in Figure 3d,e. In this configuration, a graphite disk is placed in an SS liquid holder equipped with a ceramic spacer and filled with salt (solid), as shown in Figure 3e. The liquid holder is then contained within a high-temperature furnace (Figure 3f).

The tribological testing was initiated after the temperature was held at 650°C for 30 min to ensure that the salt was melted and the temperature equilibrated. The graphite pin was then loaded onto the molten salt lubricated graphite disk and the testing was initiated. The temperature was held constant for the duration of the test. Like the dry argon sliding tests, the pin was retracted from the furnace while the disk was kept

in the furnace and allowed to cool. Solidified salt that remained on the surface of the graphite pin and disk as a residue was then washed away by sonicating in deionized water for 3 h at 35°C.

2.2.3 Wear Rate Calculation

The wear rate, K (in cubic millimeters per newton-meter), of a graphite pin and disk was calculated as the worn volume, V_{worn} (in cubic millimeters), divided by the applied normal force, F_n (in newtons), times the sliding distance, d (in meters):

$$K = \frac{V_{worn}}{F_n d}, \tag{1}$$

The worn volume V_{worn} of both graphite specimens was determined by measuring the worn surface topography using a white-light interferometer. The worn volume V_{worn} of the graphite disk was calculated as an integral of the worn surface profile $Z_{profile}$, measured at three different locations along the wear track:

$$V_{worn} = \int_0^{2\pi} \int_{R_1}^{R_2} Z(r,\theta) r dr d\theta, \tag{2}$$

where R_1 and R_2 are the left and right edge, respectively, of the profile, and r is the inner radius of the circular wear track, as shown in Figure 5.

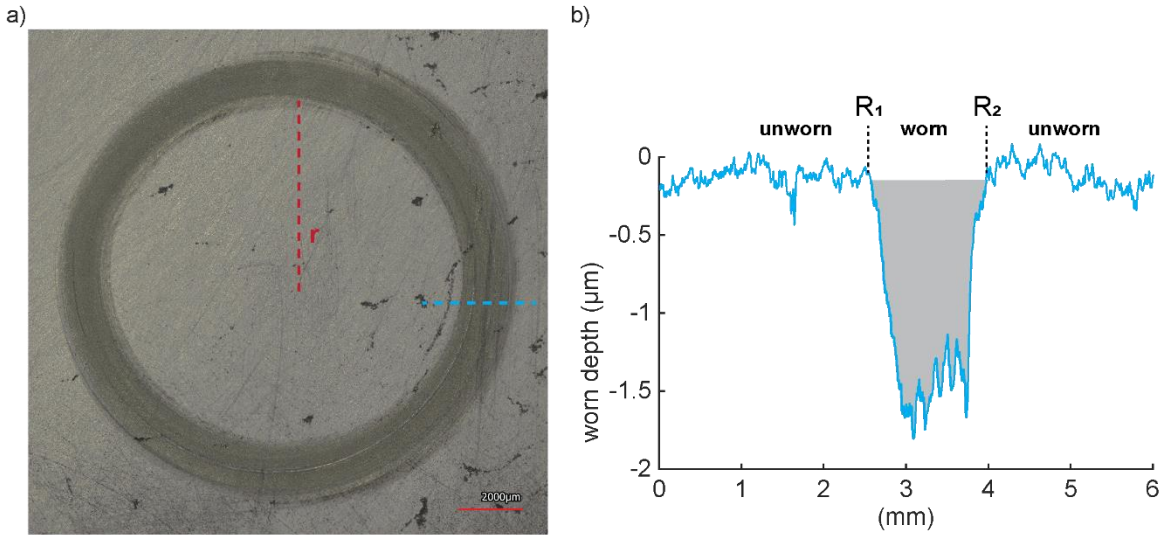

Figure 5. Disk worn surface analysis. (a) Optical image of a graphite disk after sliding at 1 mm/s in a dry argon environment. (b) Worn surface profile measured using a white-light profilometer.

The worn volume V_{worn} of the graphite pin was determined using Vision 4.10 software (Veeco Instruments, Inc.). First, the optical profilometer measured the entire worn region. The measured topography was then leveled by subtracting a spherical surface fitted to the data. The mean unworn reference plane was set to $Z = 0$ mm. The worn volume V_{worn} was then calculated by subtracting the negative volume ($Z < 0$ mm) from the positive volume ($Z > 0$ mm).

3. RESULTS AND DISCUSSION

3.1 DRY ARGON ENVIROMENT

The COF as a function of sliding distance for a graphite pin and disk pair tested at 1 mm/s and 10 mm/s sliding speeds is shown in Figure 6. The evolution of the COF is very similar for both sliding speeds. Initially, the run-in COF is higher and drops to a lower steady state after ~2 m of sliding. Lower friction and generally lower wear rate after the run-in period are typically associated with increasing the contact area and formation of a tribofilm as wear progresses. The steady-state COF is similar at both 1 and 10 mm/s sliding speeds: ~0.28 and ~0.27, respectively. However, differences are observed in the run-in friction. The COF at 10 mm/s sliding speed reached 0.58, whereas the highest COF at 1 mm/s was 0.47. Testing at slower 1 mm/s sliding speed also resulted in a faster transition to a lower steady-state COF.

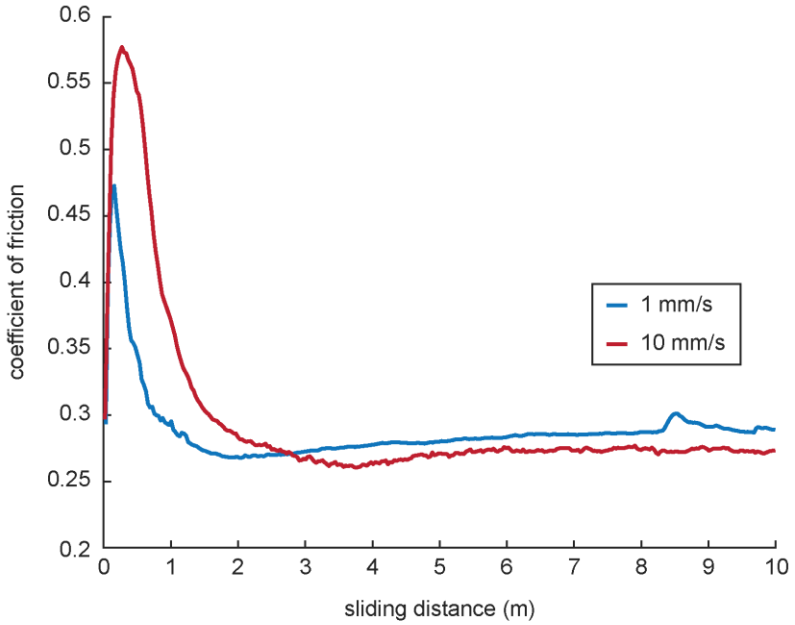

Figure 6. COF vs. sliding distance in a dry argon environment at 1 and 10 mm/s sliding speeds.

Morphological analysis of the worn surfaces showed that both graphite pin and disk exhibit abrasive wear, and the wear behavior seems to be independent of the sliding speed, as shown in Figure 7 and 8. The wear rate of the disk at 1 mm/s was 4.3×10^{-4} $mm^3/(N\text{-}m)$, which is slightly lower than the 4.7×10^{-4} $mm^3/(N\text{-}m)$ achieved at 10 mm/s, as shown in Figure 7f. On average, the depth of the wear track is around 1.5 µm for both speeds. The maximum depth of the wear track of the disk tested at 10 mm/s reaches ~2.3 µm, which was most likely caused by a surface crack, as seen in the optical images (Figure 7b) and in the worn surface topography map (Figure 7d). The graphite materials are inherently porous and could have preexisting microcracks [18], [19], and sliding could have promoted formation or extension of cracks. The wear track of the disk sample tested at 10 mm/s is also slightly wider, suggesting that the sample could have drifted during the testing. This conclusion is also supported by differences in the contrast of the wear track shown in the optical image in Figure 7d.

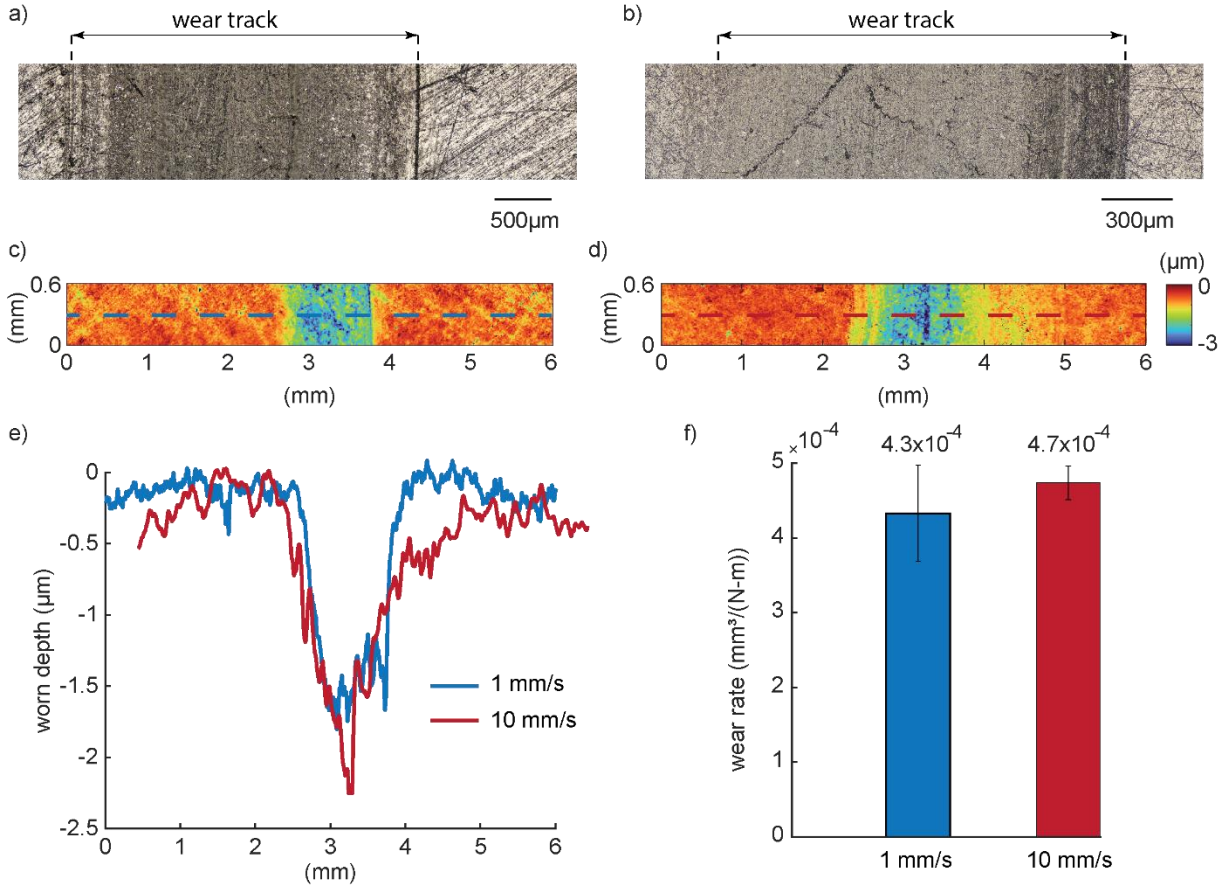

Figure 7. Analysis of worn surfaces of graphite disks in dry argon environment. Optical images of wear tracks at (a) 1 mm/s and (b) 10 mm/s sliding speeds. Worn surface topographies of wear tracks at (c) 1 mm/s and (d) 10 mm/s sliding speeds. (e) Average worn surface profiles. (f) Wear rates.

The graphite pins have similar worn surface topographies and wear rates regardless of the sliding speed, as shown in Figure 8. The optical images of worn surfaces show worn ridges that are aligned with the direction of sliding, as shown in Figure 8a,b. The darker contrast around the wear tracks indicates a deposition of wear debris. The worn profiles (Figure 8e) extracted from the worn surface topographies (Figure 8c,d) overlap each other very well. The sides of the pins facing the direction of sliding are smoother and more rounded. The wear rates of the pins at 1 and 10 mm/s are very similar: 3.9×10^{-4} mm^3/(N-m) and 4.4×10^{-4} mm^3/(N-m), respectively. The differences in the wear rates could be due to surface roughness and wear debris piling up around the wear track.

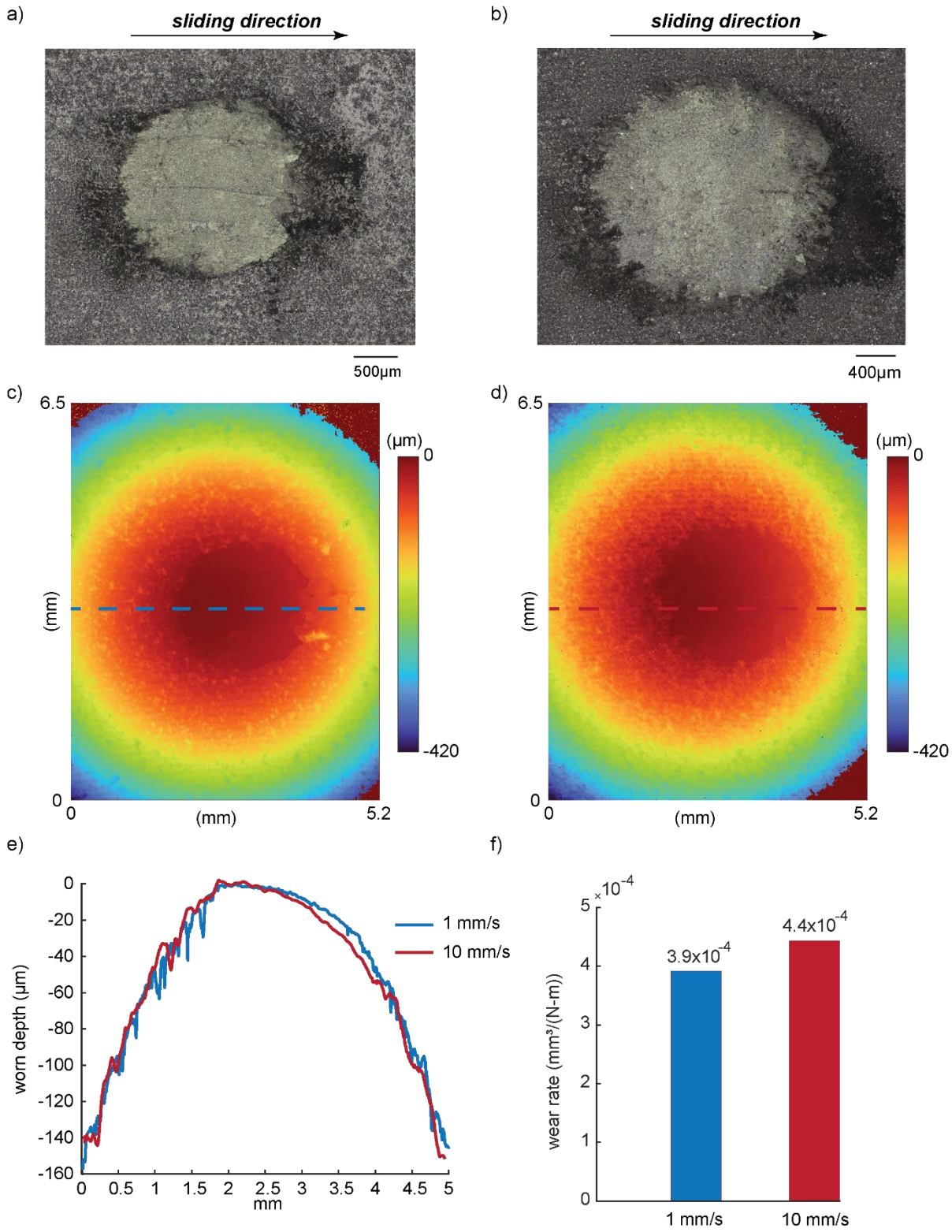

Figure 8. Analysis of worn surfaces of graphite pins in dry argon environment. Optical images of wear tracks at (a) 1 mm/s and (b) 10 mm/s sliding speeds. Worn surface topographies of wear tracks at (c) 1 mm/s and (d) 10 mm/s sliding speeds. (e) Average worn surface profiles. (f) Wear rates.

Similar tribological characterization of graphite-on-graphite sliding using a pin-on-disk configuration in an argon environment has been performed by Vergari et al. [10]. In this work, the wear and friction properties were evaluated at a range of temperatures from 17°C to 600°C, a contact load of 50 N, a sliding speed of 0.15 m/s and a sliding distance of 150 m. Although the contact load, sliding speed and temperatures are different from the ones in this work (50 vs. 20 N, 0.15 vs. 0.001–0.01 m/s, 600°C vs. 650°C), the trends in the friction behavior are similar. At 600°C, the initial run-in friction was higher; after a couple of sliding cycles, it decreases to a steady-state regime around 0.3, which is close to the values in this work. The friction data obtained at room temperature showed inconsistent behavior and, on overage, larger values.

3.2 MOLTEN FLINAK SALT ENVIRONMENT

3.2.1 Graphite-on-Graphite Sliding

In this report, the tribological testing of the graphite pin and disk pair in molten FLiNaK salt was conducted only at 10 mm/s sliding speed. The evolution of the COF was similar to the tests performed in a dry argon environment, but the values are much smaller, as shown in Figure 9. The run-in COF was ~0.14 and then dropped to a steady state of 0.07 after ~0.6 m of sliding, which is a much faster transition than in a dry argon environment.

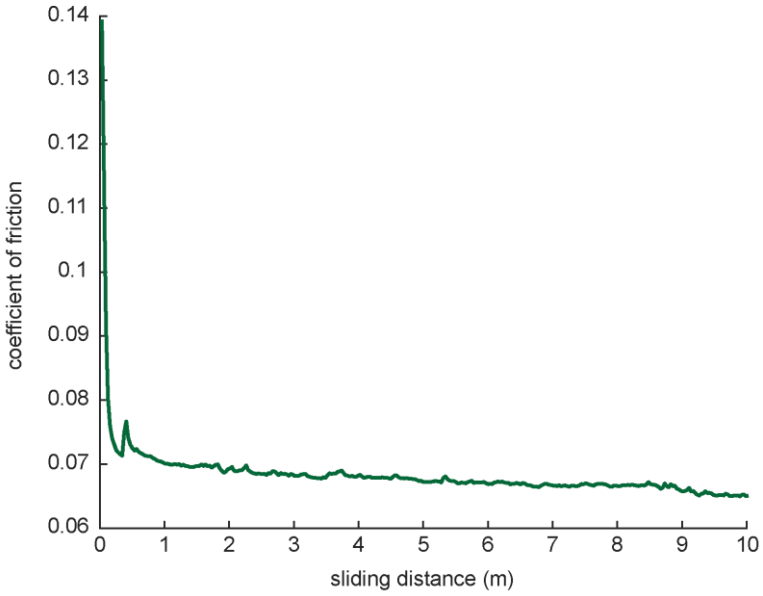

Figure 9. COF vs sliding distance in molten FLiNaK salt lubrication.

Testing in the lubricated molten FLiNaK salt conditions also improved the wear resistance. Although the wear tracks on the graphite pin and disk are visible in the optical images, they are very shallow, thus preventing a measurement of the worn volume (Figure 10).

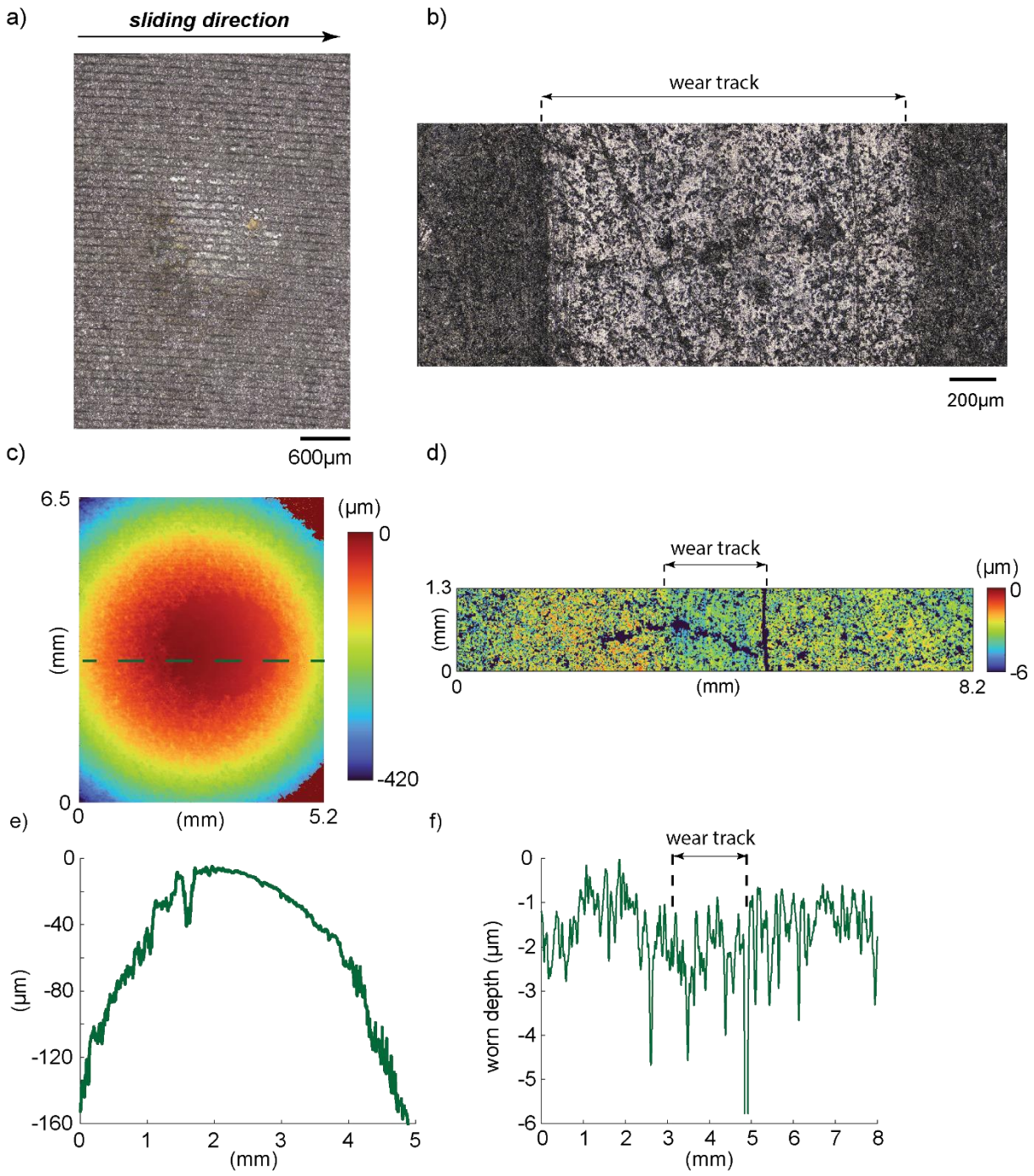

Figure 10. Analysis of worn surfaces of graphite disk and pin in molten FLiNaK salt lubrication. Optical images of wear tracks of (a) pin and (b) disk. Worn surface topographies of wear tracks of (c) pin and (d) disk. Worn surface profiles of (e) pin and (f) disk.

Molten salt provides lubricated contact between the graphite pin and the disk, thereby reducing the interfacial adhesion during sliding. This lubrication seems to provide better protection against wear and lowers the run-in and steady-state COF.

EDS elemental mapping was performed on the surface of the graphite disk to observe chemical changes on the sliding surface. The analysis showed particles composed of K and F found inside and outside the wear track, as shown in Figure 11. However, no continuous layer with K and F traces was observed, suggesting that molten FLiNaK salt was not deposited on the sliding surface. Instead, these particles are most likely salt residues that were not washed away during sonication. These particles are found only in a few regions of the wear track and are not representative of the entire worn region.

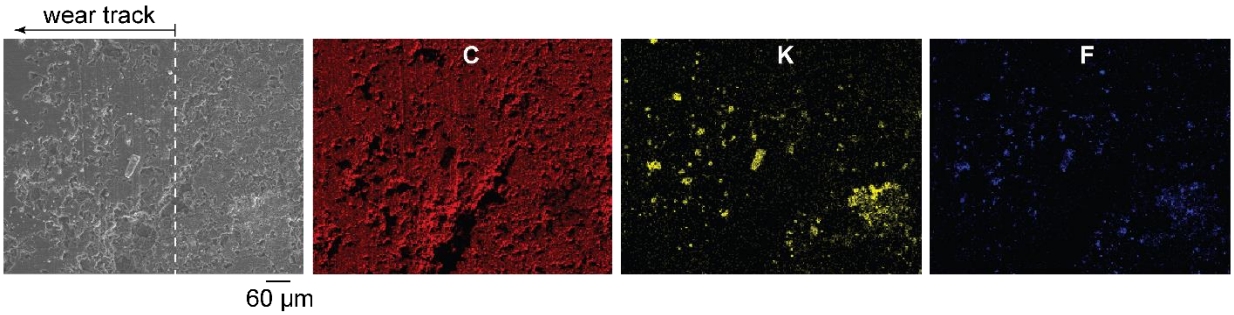

Figure 11. Elemental analysis of the worn and unworn surface of a graphite disk tested in molten FLiNaK salt.

Table 1. Maximum and steady-state COF for varying lubrication conditions and sliding speeds

Lubrication condition	Sliding speed (mm/s)	Maximum COF	Steady-state COF
Dry	1	0.47	0.28
Dry	10	0.58	0.27
Molten FLiNaK salt	10	0.14	0.07

3.2.2 Graphite on Stainless Steel Sliding

In the previous studies, the group investigated tribocorrosion of 316H SS sliding against graphite in molten FLiNaK salt (LiF:NaF:KF;46.5:11.5:42 mol %) provided by a different vendor [17]. Tribological properties were evaluated using a similar pin-on-disk configuration using a graphite pin and a 316H SS disk. This study evaluated the wear and friction properties as a function of sliding speed, temperature, and salt quantity. The results showed that a higher wear resistance and lower friction were achieved at lower temperatures (550°C vs. 650°C). This result was attributed to the lower viscosity of molten salt at a higher temperature. The tests conducted at three different sliding speeds (1, 10 and 100 mm/s) at 650°C revealed that the COF and wear rate of the graphite pin and 316H SS disk decreased with increasing sliding speed (Figure 12) because of thicker lubricant film. The effect of salt quantity on the wear and friction properties showed that, as expected, the lowest wear rate of the graphite pins was achieved with salt-flooded lubrication rather than with salt-starved and salt-free lubrication. Unexpectedly, starved lubrication resulted in the highest wear of the graphite pin and 316H SS disk. It was hypothesized that partial molten salt coverage did not provide sufficient lubrication and prevented formation of a tribofilm.

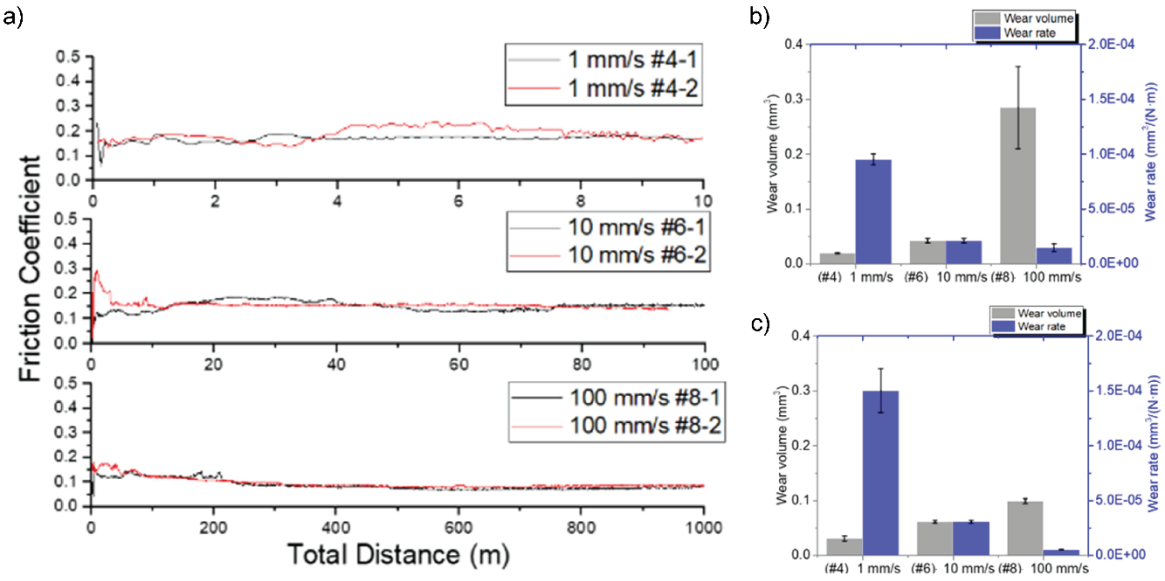

Figure 12. Graphite sliding on 316H SS in molten FLiNaK salt: effect of sliding speed. (a) Friction coefficient. (b) Wear volume and wear rate of graphite pins. (c) Wear volume and wear rate of 316H SS disks. Reproduced from [17].

4. DETERMINATION OF EXPERIMENTAL CONDITIONS AND TEST MATRIX FOR FUTURE STUDIES

Understanding tribologically relevant conditions such as the environment, contact motion, contact load, sliding speed, or sliding distance are crucial for designing the test matrix. Among these, only the environmental conditions such as temperature and gas are known; however, the other conditions must be determined.

4.1 HIGH-TEMPERATURE GAS-COOLED REACTOR

The reviewed literature on tribological testing of graphite materials in HTGRs does not provide an explanation for selecting certain experimental conditions. In a study by Vergari et al. [10], the sliding pin-on-disk experiments on E10 nuclear graphite were conducted in an argon environment, at a range of temperatures from 17°C to 600°C, contact load of 50 N, sliding speed of 0.15 m/s, and sliding distance of 150 m. Unfortunately, no explanation was given for selecting certain test parameters. Although the argon environment and the upper range of temperatures are understandable and agree with the actual conditions, the selection of the sliding speed and contact loads was not explained. In another study, tribological testing of IG-11 graphite in sliding and rolling motion by He et al. [5] were performed at the range of normal loads 390–450 N, which seems to be very high. Also, the tests were conducted at room temperature, which does not correspond to the relevant conditions.

Because the literature does not provide sufficient information about tribologically relevant conditions in an HTGR, studies that utilize a modeling approach were reviewed. Particularly, a work by Tang et al. [3] provides a detailed analysis of the pebbles' dynamics during circulation using inputs from an actual HRT-10 pebble bed reactor developed at Tsinghua University.

Modeling of a pebble flow revealed that the vertical velocity of pebbles increases toward the center and the bottom of the reactor core. Analysis of the pebble rolling motion demonstrated that the angular velocities depend on the location of the pebble in the reactor and on the relative friction between the

pebble and the wall and between the pebbles themselves. The modeling showed that the angular velocity increases with decreasing COF. Pebbles have the highest angular velocity near the wall of the reactor and at the bottom of the reactor.

The results of the sliding and rolling motion analysis suggest that the pebbles have the highest sliding and rolling speeds closer to the annulus of the reactor. Therefore, this work focused on determining the actual sliding and rolling speed values in two regions of the reactor: at the bottom wall and at the bottom center. The key simulation inputs from this study (Table 2) yielded the estimated range of sliding speeds between 1.1×10^{-4} and 1.2×10^{-3} mm/s and the estimated range of rolling speeds between 5.4×10^{-5} and 1.1×10^{-4} mm/s (Table 3). The estimated pebble sliding speeds were then used to calculate the pebble residence time to determine whether these sliding speeds agree with the actual reactor operation. The results showed that the residence time of the pebbles ranges from 20 to 185 days. According to Tang et al. [3], the average pebble residence time in HTR-10 is 207 days. This result is in good agreement with the calculated residence time at 1.1×10^{-4} mm/s pebble speed, which is around 185 days. More details about calculations of the sliding and rolling velocities can be found in Appendix A.

Contact load is another important tribologically relevant parameter. The inputs to determine a contact force on a pebble were again used from the modeling study of Tang et al. [3]. The contact load on a pebble was determined in the region close to the reactor annulus. In this approach, first, the total load of the pebbles acting on the bottom cross-sectional pebble layer was calculated. This value was then used to determine a load on a single pebble. In reality, a pebble is in contact with multiple pebbles at a time; therefore, the load is distributed. The present study assumed a configuration of five spheres, as described in Cogliati and Ougouag [4] and shown in Figure 13. The normal load acting on a pebble in the region close to the reactor annulus was then calculated to be ~28 N. More details about calculations of the contact loads can be found in Appendix A.

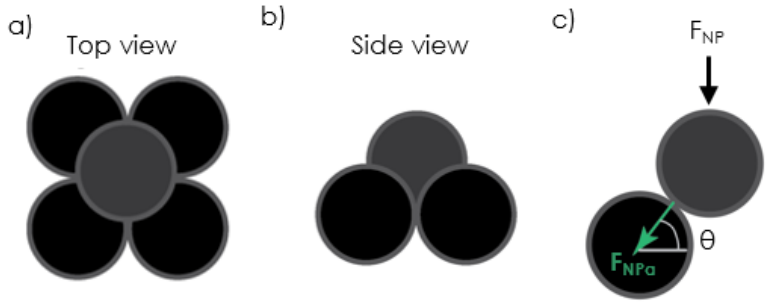

Figure 13. Simplified configuration of pebbles in the gas-cooled reactor. (a) Top view. (b) Side view, from Cogliati and Ougouag [4]. (c) Schematic of a contact between two pebbles to estimate the contact loads (Appendix A).

Table 2. Key input parameters of the analyzed gas-cooled reactor from Tang et al. [3]

Number of pebbles in reactor core	Pebble diameter (mm)	Pebble mass (g)	Reactor core diameter (m)	Reactor core length (m)
27,000	60	210	1.8	2

Table 3. Estimated contact load, sliding and rolling speeds of a pebble in a gas-cooled reactor

Contact load (N)	Sliding speed (mm/s)	Rolling speed (mm/s)
28	1.1×10^{-4}–1.2×10^{-3}	5.4×10^{-5}–1.1×10^{-4}

This analysis revealed that the rolling speeds are smaller than the sliding speeds. It is not clear which mode is more dominant, sliding or rolling. However, both speeds are extremely small to be replicated experimentally. Testing at very low sliding speeds such as <0.1 mm/s is very time-consuming and might be beyond the capabilities of the tribometer. Knowing the estimated range of sliding speeds, earlier studies involved tests at very low sliding speeds of 0.063 and 0.314 mm/s in a lab air environment at 400°C for 48 sliding cycles (equivalent of 0.6 m sliding distance), as shown in Figure 14. The evolution of the COF as a function of increasing sliding distance and the friction range were similar for both sliding speeds. The results suggest that higher sliding speeds could be used in the experimental setup. In these tests, the friction behavior did not reach a steady state; therefore, the differences in the friction at these two speeds could increase with increased sliding distance. In this work, graphite-on-graphite sliding in dry argon environment at 650°C with 1 and 10 mm/s sliding speeds exhibited similar friction behavior at both speeds (Figure 6). The only differences were observed in the initial run-in friction; however, the steady-state friction was the same. Therefore, testing at very low speeds is not necessary because the friction behavior is similar.

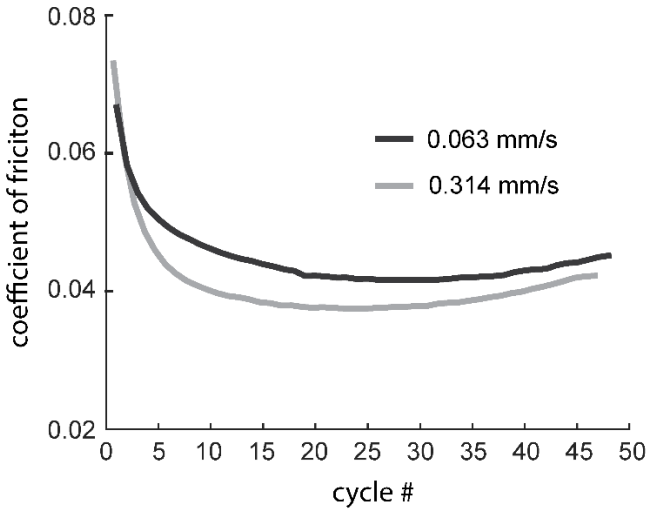

Figure 14. COF vs. sliding cycle in dry sliding for very low sliding speeds in air environment at 400°C.

4.2 MOLTEN SALT REACTOR

In MSRs, the pebbles flow in molten salt from bottom to top. This complex motion of the pebbles complicates estimating the tribologically relevant conditions such as contact loads or sliding and rolling speeds. Moreover, the literature does not provide sufficient information on dynamics of pebbles in the MSR. Fortunately, Ryan Latta and Gabriel Meric from Kairos Power agreed to provide inputs that would facilitate designing a test matrix. Kairos Power is a start-up company that focuses on developing and designing an MSR and has recently received a permit to construct its fluoride salt-cooled high-temperature Hermes reactor in Oak Ridge, Tennessee.

Based on a private discussion and data that are publicly available on the US Nuclear Regulatory Commission website [2], key inputs and factors were identified that could be used to design a test matrix to characterize tribological properties of graphite in molten salt. These data are summarized in Table 4, 5, and 6. An MSR contains approximately 36,000 pebbles, each with a diameter of 40 mm. The packing fraction of the pebbles in the reactor is 0.37. On average, pebbles pass through the reactor six times before they are discharged. One pass can take ~2–4 months. If an average pass is assumed to take 3 months and the reactor fueled length is ~3 m, then the average pebble speed is ~4×10^{-4} mm/s. This sliding speed is similar to the sliding speed of pebbles in the HTGR determined in this study (Table 3). Although pebbles

experience both rolling and sliding motion during recirculation through the reactor, rolling seems to be the more dominant contact mode based on observation from the experiments and modeling. Pebble-on-pebble contact loads vary across the reactor height. Pebbles experience the lowest contact loads/pressures at the bottom of the reactor, a few newtons, and the highest at the top before they are discharged, up to 100 N. The temperature of the molten salt ranges between 550°C and 700°C. Molten salt flow speed is 10–15 cm/s in the direction from bottom of the reactor to the top. The temperature in the reactor inlet is 550°C and 600°C–650°C in the outlet.

Table 4. Key input parameters of pebbles in the MSR, provided by Kairos Power

Number of pebbles in reactor core	Pebble diameter (mm)	Packing fraction	Pebble circulation rate	Contact load (N)
36,000	40	0.37	2–4 months/pass	<100

Table 5. Key input parameters of the MSR, provided by Kairos Power

Reactor core diameter (m)	Reactor fueled length (m)	Inlet temperature (°C)	Outlet temperature (°C)
1	3	550	600–650

Table 6. Key input parameters of molten salt used in the MSR, provided by Kairos Power

Molten salt type	Temperature (°C)	Flow rate (cm/s)
Fluoride salt	550–700	10–15

The next research efforts will focus on a more comprehensive tribological characterization of graphite in dry argon and molten salt conditions. The preliminary tribological testing, literature review, and internal discussion with Kairos Power were used to design a test matrix (Table 7). Like the preliminary testing discussed in Section 2.2.1, these tests will be conducted using the tribometer placed in a glovebox with an argon atmosphere. The primary focus will be to characterize the wear and friction properties for varying contact loads and sliding speeds while temperature and sliding distance are held constant. The tests will be performed at 20, 40, and 80 N loads because pebbles experience lower loads at the bottom of the reactor (a few newtons) and higher loads at the top of the reactor before they are discharged (up to 100 N). Two sliding speeds will be evaluated for each contact load: 1 and 10 mm/s. Testing in dry argon environment (Figure 6) showed that the steady state friction is very similar for 1 and 10 mm/s sliding speeds. It would be very useful to determine how sliding speed affects the steady state friction with molten salt lubrication. The previous studies on 316H SS sliding against graphite in molten salt lubrication showed that the steady-state friction was similar at 1 and 10 mm/s sliding speeds (Figure 12a). In the proposed tests, the temperature and sliding distance will be held constant at 650°C and 20 m.

Table 7. Proposed test matrix for tribological studies of graphite-on-graphite sliding in dry argon and molten salt conditions

Force (N)	20		40		80	
Sliding speed (mm/s)	1	10	1	10	1	10
Temperature (°C)	650	650	650	650	650	650
Sliding distance (m)	20	20	20	20	20	20

Pebble vertical speeds in an MSR and HTGR are very slow. As mentioned above, testing at such low sliding speeds is impractical. Additionally, the modeling of a pebble motion in Tang et al. [3] assumed ideal conditions in which pebbles move continuously and are uniformly distributed. However, in actual operation, the pebbles are not packed uniformly and may not move consistently. Therefore, voids (i.e., regions not occupied by pebbles) could be present in the pebble bed matrix. Situations could arise in which a pebble could move through the void and crash into an opposing pebble. In those cases, a pebble would move much faster and collide with other pebbles, resulting in an impact, rather than sliding or rolling, contact mode. In an HTGR, the movement of a pebble through the void would be downward because of gravity, whereas in an MSR, the movement would be upward in the direction of the molten salt flow, as illustrated in Figure 15. Moreover, the contact forces would be much higher than the estimated ones. Future studies will focus on determining the impact load and speed of a pebble moving through the void in both MSRs and HTGRs. Future research efforts will also attempt to characterize the tribological behavior in rolling motion. Experimental setup of a rolling motion is particularly challenging; however, He et al. [5] designed an interesting setup to characterize the wear and friction of graphite in rolling motion that seemed promising.

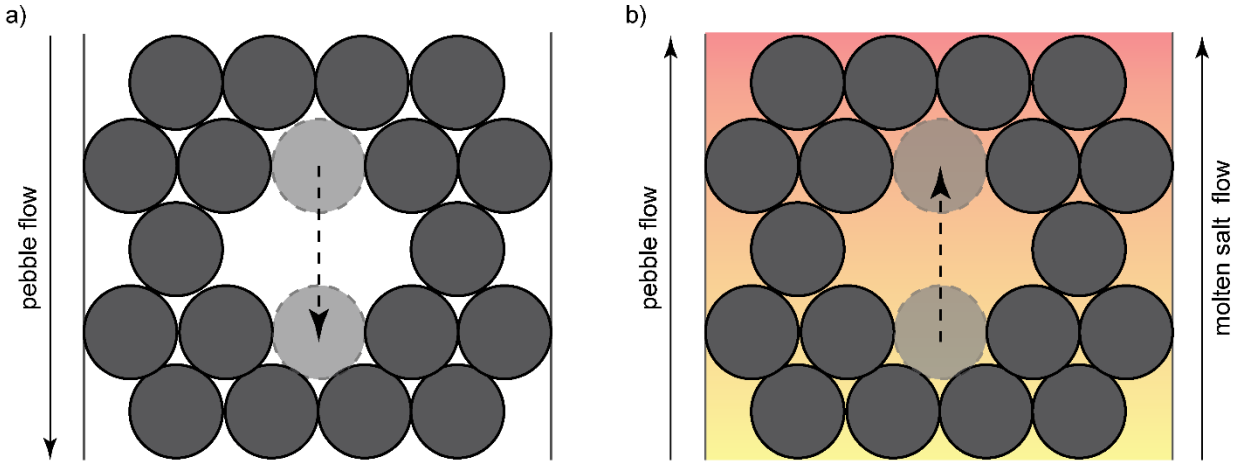

Figure 15. Schematic of a pebble moving through a void in a pebble-bed matrix. (a) In an HTGR and (b) in an MSR.

5. SUMMARY AND ONGOING WORK

This study aims to investigate the tribological behavior of graphite in HTGRs and MSRs. The approach to accomplish this goal consists of determining the tribologically relevant conditions of graphite pebbles in HTGRs and MSRs and by conducting wear and friction experiments on graphite in dry argon and molten FLiNaK salt environments. The initial tribological characterization of graphite has been performed on a multifunctional tribometer placed in a glovebox at 650°C in an argon environment. Testing in a dry argon environment showed that the friction and wear behavior of graphite was similar at 1 and 10 mm/s sliding speeds. Lubricated testing with molten FLiNaK salt resulted in much lower wear and friction, which was attributed to a reduced interfacial adhesion.

Testing in harsh environments, in this case high temperature and molten salt, presents many challenges that must be addressed. Sample holders for tribological testing are made from SS; however, molten salt is known to corrode SS materials [20], [21]. The holders would need to be replaced frequently to prevent material degradation. Another option would be to fabricate holders from corrosion-resistant alloys such as Haynes 244, which is also suitable for high-temperature applications. However, specialized alloys are significantly more expensive.

Handling fluoride salt poses another challenge. It is a hazardous substance, and improper handling may lead to health risks. The salt must be transported to the glovebox in a sealed container using proper PPE. After the completion of tribological testing, the salt solidifies on the surface of a graphite pin and disk and must be dissolved and washed away. This process complicates the analysis of the worn surface morphology and determination of the wear rates. However, molten salt can contribute to the formation of a tribofilm, and its analysis is of particular interest. Dissolving and sonicating salt from the graphite surface can prevent investigation of key morphological and chemical alterations of the sliding surface.

This report discussed designing a test matrix for more realistic characterization of the tribological properties of graphite in both HTGRs and MSRs for future studies. Inputs from simulation studies in literature and internal communication with Kairos Power were used to estimate a range of contact loads, temperature, sliding and rolling speeds, and sliding distance. Certain limitations and challenges of this study are also discussed. Particularly, lack of understanding of the pebbles' motion and interaction with other pebbles in the HTGR and MSR prevents designing a more precise test matrix to evaluate the wear and friction properties of graphite materials. As discussed in Section 4, key parameters such as pebble-on-pebble contact load/pressure, dominant contact mode, or sliding and rolling speed and distance are not known. Moreover, the pebble motion and interaction with other pebbles cannot be directly observed. Attempts were made to determine the key parameters from modeling papers. However, the simulation models often assume ideal conditions and pebble configuration, which are not necessarily representative of actual conditions in the reactor. Moreover, the contact loads and sliding/rolling speeds of the pebbles are not consistent as they pass through the reactor, which complicates design of a test matrix. The current research efforts focus on finalizing the test matrix and designing the experimental setup for rolling contact mode.

Successful completion of this project will provide much needed tribological characterization of graphite pebbles in HTGR and MSR environments. The outcomes of this work could be used to provide guidance for evaluating the integrity and service life of graphite pebbles and ensuring safe reactor operation.

6. REFERENCES

[1] M. K. M. Ho, G. H. Yeoh, and G. Braoudakis, "Molten salt reactors," *Materials and Processes for Energy, Formatex*, pp. 761–768, 2013.

[2] "https://www.nrc.gov/reactors/new-reactors/advanced/who-were-working-with/licensing-activities/pre-application-activities/kairos.html."

[3] Y. Tang *et al.*, "Analysis of the pebble burnup profile in a pebble-bed nuclear reactor," *Nuclear Engineering and Design*, vol. 345, pp. 233–251, Apr. 2019, doi: 10.1016/j.nucengdes.2019.01.030.

[4] J. J. Cogliati and A. M. Ougouag, "Pebble-Bed Pebble Motion: Simulation and Applications," Idaho State University, 2011.

[5] X. He *et al.*, "Experimental study to estimate the surface wear of nuclear graphite in HTR-PM," *Ann Nucl Energy*, vol. 116, pp. 296–302, Jun. 2018, doi: 10.1016/j.anucene.2018.02.046.

[6] E. J. Mulder and W. A. Boyes, "Neutronics characteristics of a 165 MWth Xe-100 reactor," *Nuclear Engineering and Design*, vol. 357, Feb. 2020, doi: 10.1016/j.nucengdes.2019.110415.

[7] R. S. Troy, R. V Tompson, T. K. Ghosh, S. K. Loyalka, and N. C. Gallego, "Generation of graphite particles by sliding abrasion and their characterization," *Nucl Technol*, vol. 189, no. 3, pp. 241–257, 2015.

[8] J. M. Beck and L. F. Pincock, "High Temperature Gas-Cooled Reactors Lessons Learned Applicable to the Next Generation Nuclear Plant," Idaho National Laboratory, 2011.

[9] H. Zaïdi, D. Paulmier, and J. Lepage, “The influence of the environment on the friction and wear of graphitic carbons,” *Appl Surf Sci*, vol. 44, no. 3, pp. 221–233, May 1990, doi: 10.1016/0169-4332(90)90053-3.
[10] L. Vergari, J. Quincey, G. Meric de Bellefon, T. Merriman, M. Hackett, and R. O. Scarlat, “Self-lubrication of nuclear graphite in argon at high temperature,” *Tribol Int*, vol. 177, no. September 2022, p. 107946, Jan. 2023, doi: 10.1016/j.triboint.2022.107946.
[11] X. Luo, X. Li, and S. Yu, “Nuclear graphite friction properties and the influence of friction properties on the pebble bed,” *Nuclear Engineering and Design*, vol. 240, no. 10, pp. 2674–2681, 2010, doi: 10.1016/j.nucengdes.2010.07.030.
[12] F. Robert, D. Paulmier, H. Zaïdi, and E. Schouller, “Combined influence of an inert gas environment and a mechanical action on a graphite surface,” *Wear*, vol. 181–183, pp. 687–690, Mar. 1995, doi: 10.1016/0043-1648(95)90185-X.
[13] K. Shen, J. Su, H. Zhou, W. Peng, B. Liu, and S. Yu, “Abrasion behavior of graphite pebble in lifting pipe of pebble-bed HTR,” *Nuclear Engineering and Design*, vol. 293, pp. 395–402, Nov. 2015, doi: 10.1016/j.nucengdes.2015.07.051.
[14] E. Hao *et al.*, “Influence of molten salt with or without V2O5 on hot corrosion and high-temperature tribological performance of HVOF-sprayed Ni-based self-lubricating composite coating,” *Surf Coat Technol*, vol. 417, Jul. 2021, doi: 10.1016/j.surfcoat.2021.127210.
[15] X. He, K. R. Robb, D. Sulejmanovic, J. R. Keiser, and J. Qu, “Effects of Particle Size and Concentration of Magnesium Oxide on the Lubricating Performance of a Chloride Molten Salt for Concentrating Solar Power,” *ACS Sustain Chem Eng*, vol. 9, no. 14, pp. 4941–4947, Apr. 2021, doi: 10.1021/acssuschemeng.0c09123.
[16] X. He *et al.*, “Tribological behavior of ceramic-alloy bearing contacts in molten salt lubrication for concentrating solar power,” *Solar Energy Materials and Solar Cells*, vol. 225, Jun. 2021, doi: 10.1016/j.solmat.2021.111065.
[17] X. He, C. Kumara, D. Sulejmanovic, J. R. Keiser, N. Gallego, and J. Qu, “Tribocorrosion of stainless steel sliding against graphite in FLiNaK molten salt,” *Wear*, vol. 522, no. xxxx, p. 204706, Jun. 2023, doi: 10.1016/j.wear.2023.204706.
[18] J. Moon *et al.*, “A neutron tomography study to visualize fluoride salt (FLiNaK) intrusion in nuclear-grade graphite,” *Carbon N Y*, vol. 213, Sep. 2023, doi: 10.1016/j.carbon.2023.118258.
[19] H. M. Freeman *et al.*, “On the nature of cracks and voids in nuclear graphite,” *Carbon N Y*, vol. 103, pp. 45–55, Jul. 2016, doi: 10.1016/j.carbon.2016.03.011.
[20] S. S. Raiman *et al.*, “Corrosion of 316H stainless steel in flowing FLiNaK salt,” *Journal of Nuclear Materials*, vol. 561, Apr. 2022, doi: 10.1016/j.jnucmat.2022.153551.
[21] Q. Liu *et al.*, “Corrosion behaviour of 316H stainless steel in molten FLiNaK eutectic salt containing graphite particles,” *Corros Sci*, vol. 160, Nov. 2019, doi: 10.1016/j.corsci.2019.108174.

APPENDIX A. SLIDING AND ROLLING SPEEDS AND CONTACT LOADS CALCULATIONS

The sliding and rolling velocities from the analyzed HTGR in Tang et al. [3] were determined as:

$$sliding\ velocity\left[\frac{mm}{s}\right] = \ vert.vel.\left[\frac{d}{\tau}\right]/sf, \tag{3}$$

$$rolling\ velocity\left[\frac{mm}{s}\right] = \ \omega\theta\left[\frac{1}{\tau}\right] * d/2[mm]/sf. \tag{4}$$

where d = 60 mm is the diameter of a pebble, τ = 0.0782 sec. is the simulation time scale, sf = 7.06×10^5 is the scaling factor, and vertical velocities (*vert. vel.*) were estimated to be -1.1 and -0.1 at the bottom center and the bottom wall regions, respectively from the modeling results. The values of $\omega\theta$ were determined to be 0.1 at the bottom center and 0.2 at the bottom wall regions of the reactor, from the modeling results, assuming a more realistic 0.125 friction coefficient of a pebble.

The estimated contact load on a pebble at the bottom of the analyzed reactor core analyzed in Tang et al. [3] was determined as in following steps. First, a number of pebbles in the cross-section of the reactor was calculated as a ratio of the cross-sectional areas of the reactor core (A_c) and a single pebble (A_p):

$$N_c = \frac{A_c}{A_p}. \tag{5}$$

The total load of the pebbles acting on the bottom cross-sectional pebble layer, F_{NC}, was determined as:

$$F_{NC}[N] = \ N_T * m_p[g] * g\left[\frac{m}{s^2}\right], \tag{6}$$

where N_T=27,000 is an estimated total number of pebbles acting on the bottom cross-sectional pebble layer, m=0.21 kg is a mass of a single pebble and g=9.81 (m/s^2) is the gravitational acceleration. The load on a single pebble, F_{NP}, was then calculated as:

$$F_{NP}[N] = \frac{F_{NC}}{N_C}, \tag{7}$$

The actual contact on a pebble was determined using a simplified configuration model in Figure 13, in which 4 pebbles lie on a flat surface and the fifth pebble is placed on top of them. The contact between the top and bottom pebble is at angle of 60°. Since the force from the top pebble is distributed among 4 bottom pebbles, the actual load, F_{NPa}, is determined as:

$$F_{NPa}[N] = \frac{F_{NP}}{4*cos(\theta)}. \tag{8}$$

F_{NPa} was calculated to be approximately 28 N.